Inferential framework for nonstationary dynamics. II. Application to a model of physiological signaling

Andrea Duggento,[1] Dmitri G. Luchinsky,[1,2,3] Vadim N. Smelyanskiy,[2] Igor Khovanov,[1] and Peter V. E. McClintock[1]
[1]*Department of Physics, Lancaster University, Lancaster LA1 4YB, United Kingdom*
[2]*NASA Ames Research Center, Mail Stop 269-2, Moffett Field, California 94035, USA*
[3]*Mission Critical Technologies, Inc., 2041 Rosecrans Avenue, Suite 225, El Segundo, California 90245, USA*
(Received 30 January 2008; published 4 June 2008)

The problem of how to reconstruct the parameters of a stochastic nonlinear dynamical system when they are time-varying is considered in the context of online decoding of physiological information from neuron signaling activity. To model the spiking of neurons, a set of FitzHugh-Nagumo (FHN) oscillators is used. It is assumed that only a fast dynamical variable can be detected for each neuron, and that the monitored signals are mixed by an unknown measurement matrix. The Bayesian framework introduced in paper I (immediately preceding this paper) is applied both for reconstruction of the model parameters and elements of the measurement matrix, and for inference of the time-varying parameters in the nonstationary system. It is shown that the proposed approach is able to reconstruct unmeasured (hidden) slow variables of the FHN oscillators, to learn to model each individual neuron, and to track continuous, random, and stepwise variations of the control parameter for each neuron in real time.

DOI: 10.1103/PhysRevE.77.061106 PACS number(s): 02.50.Tt, 05.45.Tp, 05.10.Gg, 05.45.Xt

I. INTRODUCTION

Time variability and nonlinearity are natural ingredients of physiological systems. In addition, a system's environment and its own internal complexity often create a strong fluctuational background that is frequently an essential feature of the dynamics. It is a context where physiological models are rarely known from first principles, and model identification and parameter inference become indispensable from the points of view of both fundamental and applied physiology [1,2] and in view of likely medical applications. In many situations, the real-time tracking of physiological parameters is the key to successful applications including, e.g., brain-controlled interfaces [3,4]. However, the interplay of noise, nonlinearity, and the time variability of the model parameters makes it difficult to extract reliable information from the data, and very difficult to do so quickly. Accordingly, the simplifying assumptions of linearity and/or determinism [2,5] are frequently made in an attempt to facilitate inference rather than on physiological grounds.

In addition, physiologically important parameters that describe specific features of the system state or system dynamics are not usually directly measurable and have to be inferred from measurements of other types of information. At present, there are no general methods available to solve this problem if the model is stochastic, nonlinear, and nonstationary, i.e., its parameters vary in time.

In paper I [6], we introduced a general Bayesian framework that allows one to identify a nonlinear stochastic model from time-series data and to infer its time-varying parameters in real time. In the present paper, we verify the approach by applying it to the analysis of a model of physiological signaling. The model chosen is a set of the FitzHugh-Nagumo (FHN) systems [7–9]. It has been found useful in analyzing dynamics of nerve fibers [10] and certain muscle cells in heart tissue [11–13]. It has also been used intensively in studies of passive myelinated axons [14] and various forms of arrythmia and cardiac activation evolution [15]. The control of such neural-related dynamics is important in the context of biotechnological applications ranging from neural models of voluntary movement [16] to studies of control in nerve conduction [17].

In our model, the measured signals corresponding to fast variables of the FHN system (e.g., action potentials) are mixed by the unknown measurement matrix. Slow variables are hidden, which is the case in most real applications. It is assumed that physiological information is coded in the time-varying control parameters η of each FHN system. Our goals will be to reconstruct the hidden variables and the measurement matrix, to learn the parameters of each individual system, and to use this information for extracting the time variation of the control parameter η in real time. We will show, in particular, that the approach is able to decode large stepwise changes, as well as random and continuous variations of the control parameter, for each oscillator in real time. Furthermore, we will show that the parameter-tracking algorithm can effectively be embedded into the inferential learning framework, enabling us to reconstruct both the unmeasured (hidden) variables of the FHN oscillators and the model parameters. For simplicity, we will assume that FHN systems are not coupled and that the dynamical equation for the slow variable does not include a random force. However, both coupling and noise in the hidden variables can be incorporated into the method, as will be shown elsewhere.

The paper is organized as follows. In Sec. II, a model of FHN systems coupled by an unknown measurement matrix is presented and then reduced to standard form suitable for analysis within the Bayesian framework. Convergence of the model parameters for the case of stationary signals is discussed in Sec. III. Their convergence and online tracking when the system is nonstationary are presented in Sec. IV. Finally, the results obtained are summarized and conclusions are drawn in Sec. V.

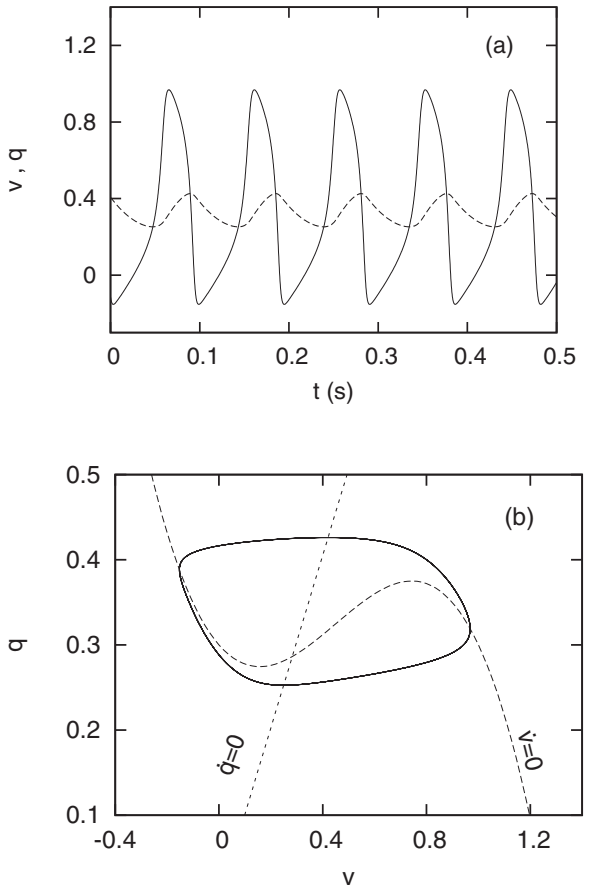

FIG. 1. Numerical simulation of the FitzHugh-Nagumo oscillator (1). (a) Examples of the time traces of v_j (solid line) and q_j (dashed line). (b) Nullclines are shown by the dashed (first equation) and dotted (second equation) lines, and the corresponding phase trajectory is shown by the thin solid line.

II. SYSTEM OF FITZHUGH-NAGUMO OSCILLATORS

In a typical physiological situation, neurons fire at the rate of $\sim 5-10\ \mathrm{s}^{-1}$. The correlation time of the control parameter is $\sim 500-1000$ ms. The correlation times of other model parameters in the nonstationary case are ~ 5 s. A typical sampling rate for measurements is ~ 20 kHz. In order to follow the time variations, it is necessary for the computation time to be less than the shortest characteristic time in the system, i.e., that for variation of the control parameters. So we must aim for a computational inference delay time of less than 500 ms.

To model this spiking activity, we use the well-known FitzHugh-Nagumo system in the form

$$\dot{v}_j = -v_j(v_j - \alpha_j)(v_j - 1) - q_j + \eta_j + \sqrt{D_{ji}}\xi_i,$$

$$\dot{q}_j = -\beta q_j + \gamma_j v_j,$$

$$\langle \xi_j(t)\xi_i(t')\rangle = \delta_{ij}\delta(t-t'), \quad j = 1{:}L. \tag{1}$$

This system (1) represents the simplified dynamics of L noninteracting neurons [8], where v_j model the membrane potentials and q_j are slow recovery variables. Figure 1 illustrates the dynamics for one oscillator in the absence of noise; values of the other parameters are $\alpha=0.4$, $\eta=0.3$, $\beta=0.0151$, and $\gamma=0.0153$.

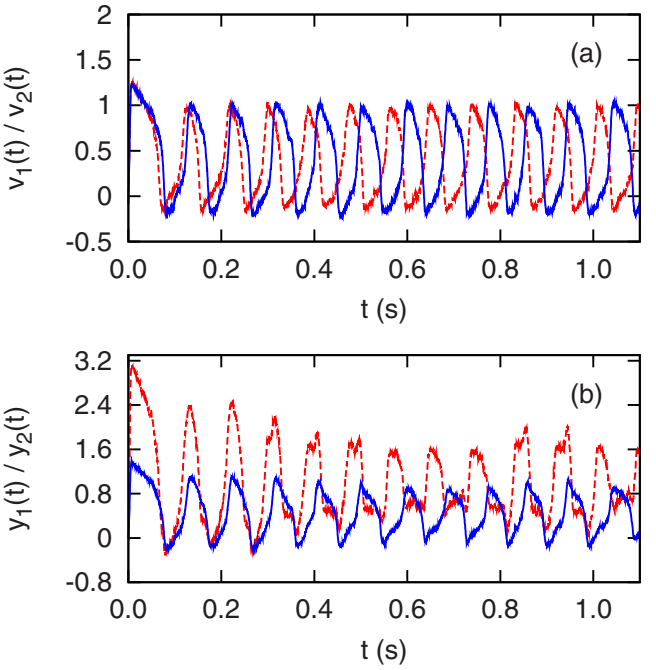

FIG. 2. (Color online) Time-series data generated by the model (1),(2) (a) before and (b) after mixing, for the parameters given in Table I. Parameters η_1 and η_2 fluctuate between 0.35 and 0.45. The dotted (red) lines show $v_1(t)$ and $y_1(t)$ and the solid (blue) lines show $v_2(t)$ and $y_2(t)$.

We assume that the important physiological information is encoded in the parameters η_i, which control the frequency of firing. In practice, this information is difficult to extract because signals collected from biological systems are noisy and often mixed with an unknown measurement matrix. To analyze the situation in a realistic way, we introduce dynamical noise into the model system (1) and a measurement matrix $\boldsymbol{X}$ into the following measurement model:

$$y_i = X_{ij}v_j. \tag{2}$$

Here y_i are measured variables, related to v_j by linear transformation with the *unknown* matrix $\boldsymbol{X}$. An example of noisy signals before and after the mixing is shown in Fig. 2. We suppose that the only accessible information is contained in y_i. The problem is therefore to learn the model parameters $\mathcal{M}=\{\eta_i,\alpha_i,q_i(0),\gamma_i,D_{ij},X_{ij}\}$ from the time-series data $\{y_i\}$, and to use this information for fast on-line tracking of the time-varying parameters $\{\eta_i\}$ for each neuron. It was shown in paper I that this problem can be treated within a general inferential framework by integrating the middle set of equations in Eqs. (1) to obtain

$$q_j(t) = \gamma_j \int_0^t d\tau e^{-\beta(t-\tau)}v_j(\tau) + e^{-\beta t}q_j(0). \tag{3}$$

On substituting Eq. (3) into the top equation in Eqs. (1), we have

$$\dot{v}_j = -\alpha_j v_j + (1+\alpha_j)v_j^2 - v_j^3 + \eta_j - \gamma_j \int_0^t d\tau e^{-\beta(t-\tau)} v_j(\tau) - e^{-\beta t} q_j(0) + \sqrt{D_{ij}}\xi_j. \quad (4)$$

Here $j=1,\ldots,L$, and $q_j(0)$ is a set of initial coordinates for the unobservable variable $q_j(t)$. Thus the reconstruction of unobservable variables $q_j(t)$ is reduced to the inference of the L initial conditions $q_j(0)$.

Furthermore, the variables $v_j(t)$ can also be excluded from further consideration by using Eq. (2). On substituting $\boldsymbol{v}=\boldsymbol{X}^{-1}\boldsymbol{y}$ into Eq. (4), we obtain in vector notation

$$\dot{\boldsymbol{y}} = \boldsymbol{X}\boldsymbol{\alpha}(\boldsymbol{X}^{-1}\boldsymbol{y}) + \boldsymbol{X}(\mathbf{1}+\boldsymbol{\alpha})(\boldsymbol{X}^{-1}\boldsymbol{y})^2 + \boldsymbol{X}(\boldsymbol{X}^{-1}\boldsymbol{y})^3 + e^{-\beta t}\boldsymbol{X}\boldsymbol{q}_0 - \int_0^t e^{\beta(t-\tau)}\boldsymbol{X}\boldsymbol{\gamma}(\boldsymbol{X}^{-1}\boldsymbol{y})d\tau + \boldsymbol{X}\boldsymbol{\eta} + \boldsymbol{X}\sqrt{\boldsymbol{D}}\boldsymbol{\xi}(t), \quad (5)$$

where $q_0=q(t=0)$, $\boldsymbol{\alpha}$ and $\boldsymbol{\gamma}$ are matrices with α_i and γ_i on the respective diagonals, and

$$(\boldsymbol{X}^{-1}\boldsymbol{y})^n = \begin{pmatrix} \left(\sum_{i=1}^L x_{1i}y_i\right)^n & \cdots & 0 \\ \vdots & \ddots & \vdots \\ 0 & \cdots & \left(\sum_{i=1}^L x_{Li}y_i\right)^n \end{pmatrix}.$$

Here x_{ij} are elements of the inverse matrix $\boldsymbol{X}^{-1}$.

The advantage of the presentation (5) is that it allows for the fastest on-line tracking of the control parameters of the system (1) in the case of small measurement noise. In what follows, we demonstrate this point using as an example a system of two FHN oscillators. However, the results reported below can be readily extended to a set of L linearly coupled FHN systems. We will refer to system (5) as "transformed dynamics" to distinguish it from the "reduced dynamics" of Eq. (4).

III. STATIONARY DYNAMICS AND CONVERGENCE

To infer the parameters of the system of L FHN oscillators (5) within the stationary regime, we introduce the following base functions:

$$\phi(x) = \{\mathbf{1}, y_1, \ldots, y_L, y_1^2, y_1y_2, \ldots, y_1y_L, y_2^2, y_2y_3, \ldots, y_2y_L, \ldots, y_1^3, y_1^2y_2, \ldots, y_1^2y_L, y_2^3, y_2^2y_1, \ldots, y_2^2y_L, \ldots, y_L^2y_{L-1}, y_L^3, \Phi_1, \ldots, \Phi_L, e^{-\beta t}\}, \quad (6)$$

where Φ_i is defined as follows:

$$\Phi_i \equiv \int_0^t y_i(\tau)e^{\beta(\tau-t)}d\tau.$$

The number of base functions,

$$N_\phi = 2 + 2L + \frac{L(L+1)}{2} + L^2, \quad (7)$$

increases as L^2 with the number of systems. The number of unknown coefficients of the system (5) is $N_c=N_\phi\times L+L^2+\frac{L(L+1)}{2}$; it increases as L^3 with the dimension of the system. The first term in N_c is the full set of unknown coefficients, because all possible combinations of the powers of y are included in this set, i.e., it covers the whole model space of the system with polynomial base functions up to power 3. The second term in N_c is the number of unknown elements of the measurement matrix $\boldsymbol{X}$, while the third is the number of elements of the unknown noise matrix. Only $N_{\inf}=N_\phi\times L+\frac{L(L+1)}{2}$ coefficients can be inferred directly from the time-series data $\{y_i\}$, and therefore only $N_{\inf}$ equations can be formed to find the coefficients of the original system (4) and the elements of the matrix $\boldsymbol{X}$. In practice, however, the number of coefficients of the original system is always significantly smaller than the full set $N_{\inf}$, because of the symmetry that is always present in real systems. In particular, the number of unknown coefficients in the original system (2), (4) is $N_{\mathcal{M}}=6L+L^2+\frac{L(L+1)}{2}$ (note that here we have counted coefficients for y_i^2 and y_i^3). That is, for a system of two FHN oscillators we have $N_{\inf}=29$ equations to reconstruct $N_{\mathcal{M}}=19$ coefficients.

So it should be possible at least in principle to reconstruct all unknown coefficients of the original system for any number of FHN oscillators, provided that we can establish the connection between the set

$$\tilde{\mathcal{M}} = \{\tilde{\eta}_i, \tilde{\alpha}_{ij}, \tilde{b}_{ijk}, \tilde{c}_{ijkl}, \tilde{\gamma}_{ij}, \tilde{q}_i(0), \tilde{D}_{ij}\}$$

of measured variables of the transformed system (5) and the set

$$\mathcal{M} = \{\eta_i, \alpha_i, b_i, c_i, \gamma_i, q_i(0), D_{ij}, X_{ij}\}$$

of unknown parameters of the original reduced dynamics (4), where $b_i=(\alpha_i+1)$ and $c_i=-1$. Note that the coefficients $\tilde{\alpha}_{ij}$, $\tilde{b}_{ijk}$, $\tilde{c}_{ijkl}$, and $\tilde{\gamma}_{ij}$ in the expression for $\tilde{\mathcal{M}}$ above correspond to the coefficients A_{ij}, B_{ijk}, C_{ijkl}, and Γ_{ij} in Eqs. (36), (37) of paper I. In the two-dimensional (2D) case, the set $\tilde{\mathcal{M}}$ of variables of the transformed dynamics (5) corresponds to the following set of base functions:

$$\phi(x) = \{\mathbf{1}, y_1, y_2, y_1^2, y_2^2, y_1y_2, y_1^3, y_1^2y_2, y_1y_2^2, y_2^3, \Phi_1, \Phi_2, e^{-\beta t}\}. \quad (8)$$

Once parameters of the transformed dynamics are inferred, one has to reconstruct parameters of the original model (1). In general form, the connection between the two sets of coefficients is given by Eqs. (37)–(39) of paper I. Here we introduce explicit relations for the case $L=2$,

$$\boldsymbol{X}^{-1}\begin{bmatrix}\eta_1\\ \eta_2\end{bmatrix} = \begin{bmatrix}\tilde{\eta}_1\\ \tilde{\eta}_2\end{bmatrix}, \quad (9)$$

$$\begin{bmatrix}q_{0,1}\\ q_{0,2}\end{bmatrix} = \boldsymbol{X}^{-1}\begin{bmatrix}\tilde{q}_1\\ \tilde{q}_2\end{bmatrix}, \quad (10)$$

$$\begin{bmatrix}\gamma_1 & 0\\ 0 & \gamma_2\end{bmatrix}\boldsymbol{X}^{-1} = \boldsymbol{X}^{-1}\begin{bmatrix}\tilde{\gamma}_{11} & \tilde{\gamma}_{12}\\ \tilde{\gamma}_{21} & \tilde{\gamma}_{22}\end{bmatrix}, \quad (11)$$

$$\begin{bmatrix}\alpha_1 & 0\\ 0 & \alpha_2\end{bmatrix}\boldsymbol{X}^{-1} = \boldsymbol{X}^{-1}\begin{bmatrix}\tilde{\alpha}_{11} & \tilde{\alpha}_{12}\\ \tilde{\alpha}_{21} & \tilde{\alpha}_{22}\end{bmatrix}, \quad (12)$$

$$\tilde{\boldsymbol{D}}\boldsymbol{X}^{-1} = \boldsymbol{X}^{-1}\boldsymbol{D}. \tag{13}$$

The unknown elements x_{ij} of the inverse measurement matrix $\boldsymbol{X}^{-1}$, and the parameters with tildes, are the model parameters of the transformed system (5) that can be inferred directly using time-series data $\{y_i\}$. Relations (9)–(13) allow one to reconstruct 15 unknown parameters of the original system, including elements of the noise and measurement matrices. Note, however, that the coefficients $(1+\alpha_i)$ can also be assumed unknown in general and that the following relations can be used to reconstruct them:

$$\begin{bmatrix} 1+\alpha_1 & 0 \\ 0 & 1+\alpha_2 \end{bmatrix} \begin{bmatrix} x_{11}^2 & 2x_{11}x_{12} & x_{12}^2 \\ x_{21}^2 & 2x_{21}x_{22} & x_{22}^2 \end{bmatrix} = \boldsymbol{X}^{-1} \begin{bmatrix} \tilde{b}_{111} & \tilde{b}_{112} & \tilde{b}_{122} \\ \tilde{b}_{211} & \tilde{b}_{212} & \tilde{b}_{222} \end{bmatrix}. \tag{14}$$

Similarly, the relationships between the coefficients for polynomials of power 3 are given by

$$\begin{bmatrix} -1 & 0 \\ 0 & -1 \end{bmatrix} \begin{bmatrix} x_{11}^3 & 2x_{11}^2x_{12} & 2x_{11}x_{12}^2 & x_{12}^3 \\ x_{21}^3 & 2x_{21}^2x_{22} & 2x_{21}x_{22}^2 & x_{22}^3 \end{bmatrix} = \boldsymbol{X}^{-1} \begin{bmatrix} \tilde{c}_{111} & \tilde{c}_{112} & \tilde{c}_{121} & \tilde{c}_{122} \\ \tilde{c}_{211} & \tilde{c}_{212} & \tilde{c}_{221} & \tilde{c}_{222} \end{bmatrix}, \tag{15}$$

Note that in general one could introduce unknown parameters for the coupling between the FHN systems and use relations similar to Eqs. (12), (14), and (15) to reconstruct these parameters. Note also that it is a simple matter to extend Eqs. (9)–(15) to encompass the L-dimensional case.

In the new notation, the two-dimensional equations for the reduced dynamics take the form

$$\dot{y}_i = \tilde{\eta}_i + \tilde{\alpha}_{ij}y_j + \tilde{b}_{ik_1k_2}y_{k_1}y_{k_2} + \tilde{c}_{ik_1k_2}y_{k_1}y_{k_2}^2 + e^{-\beta t}\tilde{q}_i - \gamma_{ij}\int_0^t e^{\beta(t-\tau)}y_j d\tau + \sqrt{\tilde{D}_{ij}}\xi_j(t), \tag{16}$$

Equation (16) with the $N_\phi = 13$ base functions (8) allows one to apply explicitly the results of paper I [6] to infer the $N_{\text{inf}} = 29$ parameters of the transformed system (16). Indeed, the base functions (8) and the model parameters in Eq. (16) can be used to factorize the vector field according to Eqs. (7) and (8) of [6]. The minus log-likelihood function and its gradient for the transformed system (16) can then be written using Eqs. (6) and (26) of [6]. At the next step, Eqs. (10)–(14) of the main algorithm of [6] can be used to reconstruct the model parameters of the transformed system. Once the parameters of the transformed system have been inferred, one can use Eqs. (9)–(13) to reconstruct the parameters of the original model (1).

In the rest of this section, we restrict ourselves to the 2D case and analyze the convergence of the method under stationary conditions. Our goals will be to show the correlation between the convergence of the model parameters and the decay of the eigenvalues $\{\lambda_i\}$ of matrix $\hat{\boldsymbol{\Xi}}^{-1}$ (see paper I), and to demonstrate how one can speed up the convergence by orders of magnitude by reducing the number of base functions in an appropriate way.

TABLE I. Parameter values of the model (1), (2) used to generate stationary time-series data.

$\alpha_1 = 0.35$	$\eta_1 = 0.4$
$\alpha_2 = 0.20$	$\eta_2 = 0.3$
$\gamma_1 = 0.0153$	$\beta = 0.0151$
$\gamma_2 = 0.0153$	
$d_{11} = 0.0002$	$d_{12} = 0.00007$
$d_{22} = 0.0002$	$d_{21} = 0.00007$
$x_{11} = 1.7$	$x_{12} = 0.8$
$x_{22} = 0.2$	$x_{21} = 0.9$

A. Convergence of the parameters of the transformed dynamics

In this section, we analyze the convergence of the model parameters of the reduced dynamics (4) as a function of $T = hN$, where h is the sampling time step and N is the number of points in a block of data. The model (1) and (2) was integrated using the Heun scheme [18] with the set of parameters shown in Table I. The fast variables of the FHN oscillators $v_1(t)$ and $v_2(t)$ were mixed by the measurement matrix $\boldsymbol{X}$ to generate synthetic time-series data $y_1(t)$ and $y_2(t)$ of measured signals. The latter signals were used as the input for testing the algorithm. An example of the signals $v_1(t), v_2(t)$ and $y_1(t), y_2(t)$ is shown in Fig. 2.

We now analyze the convergence of the method in the case in which all parameters of the reduced model (5), including elements of the measurement matrix, are unknown. An example of the convergence of parameters for the reduced model is shown in Fig. 3. The sampling rate was 35 kHz. We used nine blocks of data with 5000 points in each block, and these blocks of data were generated at random 1000 times to analyze the statistics of the convergence. The results of the inference are summarized in Table II. It can be seen that convergence of better than 3.5% is achieved in less then 1 s, even though the coefficients of the highest order polynomials are assumed unknown.

B. Reconstruction of the mixing matrix

To reconstruct both the mixing matrix $\boldsymbol{X}$ and the parameters of the original system $\mathcal{M}$ from the inferred parameters $\tilde{\mathcal{M}}$ of the transformed system (5), we have to solve Eqs. (9)–(13) with respect to elements of $\tilde{\mathcal{M}}$. We note that, in the general case of the measurement model, these equations are nonlinear and can be written implicitly as $F_k(\mathcal{M}) = 0$, $k = 1, \ldots, K$, where K is the number of equations. In the particular case of transformation given by the simple form of Eqs. (9)–(13), the solution of this problem can be found by using the standard nonlinear least-squares method [19], although an additional optimization over the set of initial values may be required. We stress that the present technique is

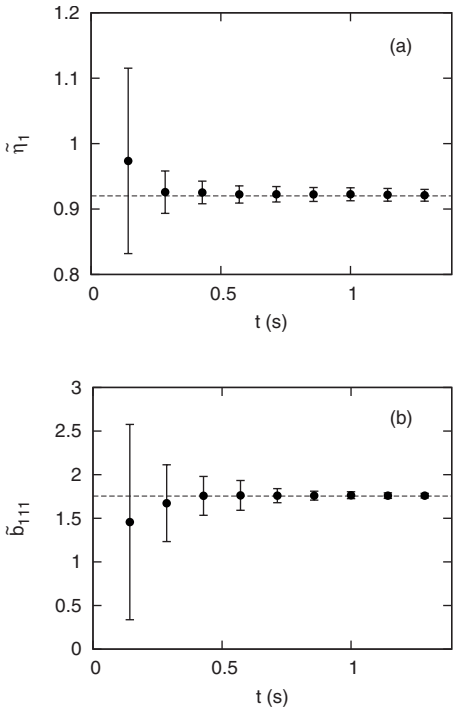

FIG. 3. Typical example of the convergence of parameters as a function of signal length. $\tilde{\eta}_1$ and $\tilde{b}_{222}$ are plotted as functions of time, i.e., of the number of data. The first point corresponds to a block of 5000 data points; each successive point corresponds to an additional 5000 data, as discussed in the text. Vertical bars show standard deviations of the inferred values, calculated over 1000 realizations. The horizontal dashed lines indicate the true values of the model parameters as given in Tables I and II.

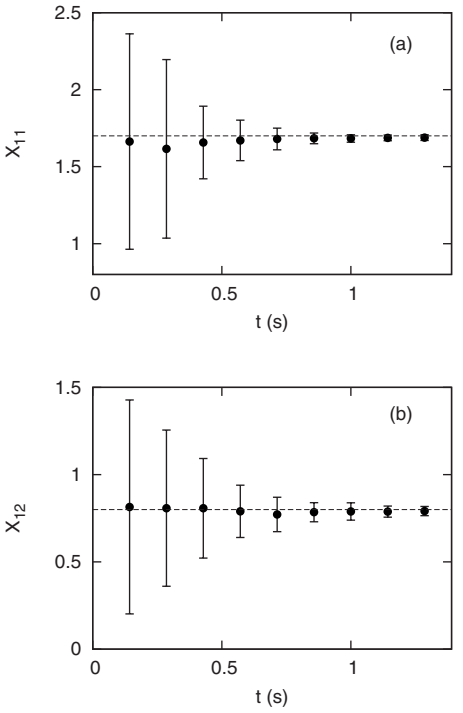

FIG. 4. (a) and (b) Typical examples of convergence for two components of the measurement matrix $\boldsymbol{X}$ as a function of the measurement time t. The model parameters for this numerical test are given in Table I. We have used nine data blocks with 5000 points in each block. The standard deviations of the inferred parameters shown by the vertical bars are calculated over 1000 realizations. The horizontal lines show the true values of the model parameters. The sampling rate was 35 kHz.

not restricted to the 2D case and can equally be applied to the general case of N FHN oscillators.

We can now use the inferred parameters of the transformed dynamics (preceding subsection, Fig. 3 and Table II) to reconstruct both the elements of the measurement matrix and the model parameters of the original system (4). Examples of convergence of the model parameters and of the elements of the measurement matrix are given in Figs. 4 and 5, and are summarized in Table III. It can be seen from the table that a relative error of inference of better than 2% is achieved within less than 1 s of measurement time.

In what follows, we will focus on the convergence of the control parameters η_i and analyze the accuracy and speed of the convergence under various assumptions about the time dependence of these parameters and information available about other parameters of the system.

TABLE II. Values of some of the original coefficients inferred using 30 000 points. The actual values (second column) are compared with the inferred values (third column); standard deviations are given in the last column.

Parameter	Real	Inferred	Std. dev.
$\tilde{\eta}_1$	0.9200	0.924384	0.022624
$\tilde{\eta}_2$	0.3500	0.351001	0.009063
$\tilde{b}_{222}$	1.7550	1.758011	0.037047
$\tilde{b}_{112}$	−2.1086	−2.114731	0.068268

C. Convergence speed

We note that the calculation of the rate of convergence of model parameters of stochastic nonlinear dynamical systems is, in general, still an open problem. Here we provide a brief discussion, however, based on the results of Sec. II C of paper I [6]. These indicate that the eigenvalues of the matrix $\hat{\boldsymbol{\Xi}}$ [see Eq. (22) of paper I] play an important role in the convergence of the model parameters. The meaning of the matrix $\hat{\boldsymbol{\Xi}}$ is twofold: first, $\hat{\boldsymbol{\Xi}}$ is the covariance of the posterior density, so it measures directly how sharply this distribution is peaked about its mean value; second, $\hat{\boldsymbol{\Xi}}$ is proportional to $\hat{\mathbf{D}} \otimes \hat{\boldsymbol{\Phi}}_k^{-1}$ [see Eq. (22) of paper I], so it is directly influenced by the choice of the base functions and by the correlations between them. It is clear, in particular, that in the case of polynomial base functions, the lower the order of polynomials, the smaller will be the eigenvalues of $\hat{\boldsymbol{\Xi}}^{-1}$, and the faster will be their convergence. Indeed, the deviation of the model parameters from their limiting mean values is proportional to a linear combination of the eigenvalues λ_i of $\hat{\boldsymbol{\Xi}}^{-1}$. So the convergence of the model parameters is determined by the values and decay rates of the largest eigenval-

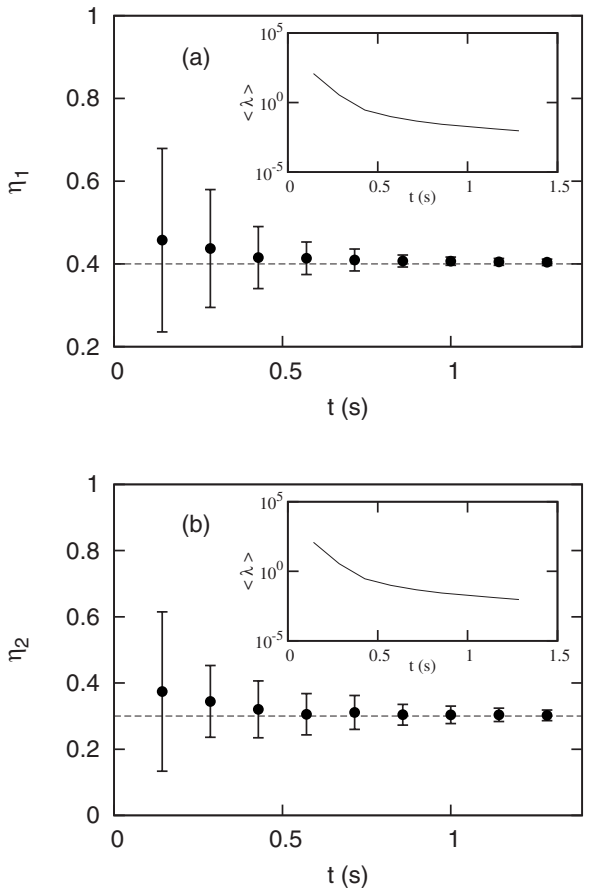

FIG. 5. (a) and (b) Convergence of the control parameters η_1 and η_2 as functions of the measurement time t. Values of the model parameters for this numerical test are given in Table I. We have used nine data blocks with 5000 points in each block. The standard deviations of the inferred parameters shown by the vertical bars are calculated over 1000 realizations. The horizontal lines show the true values of the control parameters. The sampling rate was 35 kHz. The insets in both figures show the decay of the largest eigenvalue of $\hat{\Xi}^{-1}$.

ues of $\hat{\Xi}^{-1}$. The latter in turn depend on the *a priori* information available about the model parameters. For the polynomial base functions, which is the case of transformed dynamics (5), the most important information from the point of view of convergence speed is knowledge of the coefficients for the polynomials of higher order.

To illustrate this point, we calculate the eigenvalues of $\hat{\Xi}^{-1}$ under various assumptions about the number of known parameters in the model. The results of this analysis are shown in Fig. 6. It can be seen from the figure that when no information is available about model parameters (i.e., all the parameters are unknown), the largest eigenvalue of $\hat{\Xi}^{-1}$ has an initial value of the order 10^2 and decays to 10^{-2} over a measurement time $t=1.3$ s. The correlation between the decay of the largest eigenvalue and the convergence of the η parameters in this case is evident from Fig. 5. When the coefficients of the cubic and quadratic terms in system (4) are known, the value of the largest λ_i of $\hat{\Xi}^{-1}$ (shown by the blue dashed line in Fig. 6) is reduced by three orders of magnitude. When all parameters of the system (4) are known except the control parameters η_i, the largest value of λ_i of $\hat{\Xi}^{-1}$ (shown by the black dotted lines in Fig. 6) is further reduced by two orders of magnitude.

TABLE III. Values of some of the original coefficients inferred using 30 000 points obtained from measurement matrix and real parameter reconstruction. The actual values (second column) are compared with the inferred values (third column); relative errors are given as percentages in the last column.

Parameter	Real	Inferred	Rel. error
X_{11}	1.7	1.686459	0.796526
X_{12}	0.8	0.794263	0.717092
X_{21}	0.2	0.196746	1.626811
X_{22}	0.9	0.898222	0.197610
η_1	0.4	0.406227	1.556788
η_2	0.3	0.302462	0.820660
α_1	−0.35	−0.351992	0.569082
α_2	−0.2	−0.200376	0.188228
b_1	1.35	1.357427	0.550145
b_2	1.2	1.203863	0.321885
c_1	−1.0	−0.999520	0.047957
c_2	−1.0	−0.999114	0.088582

In the latter case, convergence of the inferred parameters η_i to their true values is much faster. To verify this point, the following test was performed: (i) first a signal of length 1 s was generated with stationary dynamics and used to infer all the model parameters; (ii) next, the parameters η_i were changed in a steplike manner; and (iii) the convergence of the inferred parameters η_i was analyzed as a function of the length of the step. The results are shown in Fig. 7. It is

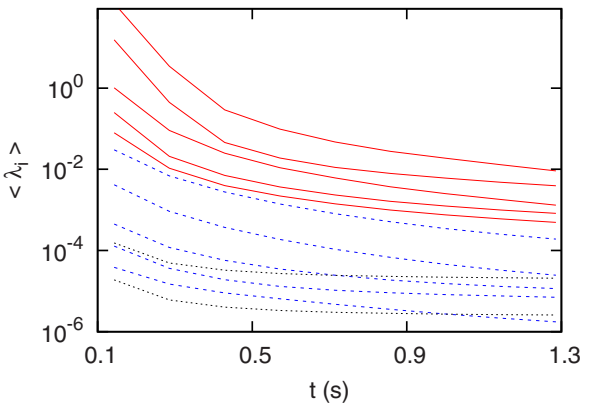

FIG. 6. (Color online) The largest eigenvalues λ_i of the matrix $\hat{\Xi}^{-1}$ under different assumptions: (i) when none of the coefficients of the dynamics in Eq. (4) are known (full red lines); (ii) when the coefficients of the third and second powers are known (dashed blue lines); (iii) when all parameters except η_i are known (dotted black lines). The dynamical coefficients are the same as in Fig. 4. The number of runs to obtain the averaged convergence was 1000 for each data block size. The actual distribution for each eigenvalue is highly asymmetric over the number of the runs, and typical values of λ_i are lower than their respective means.

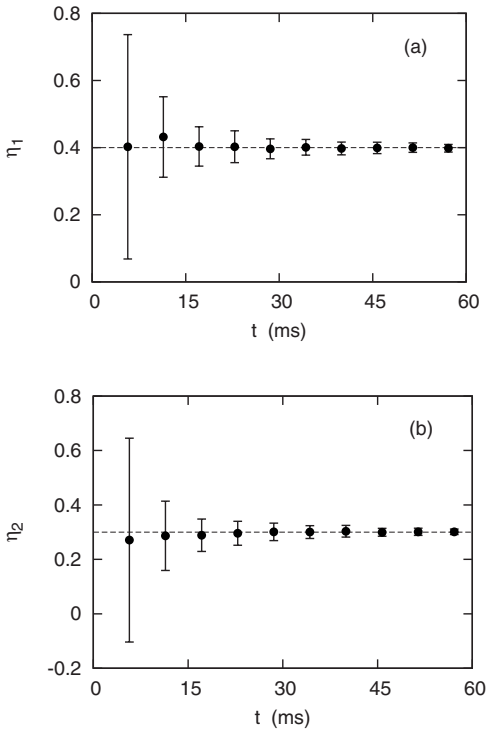

FIG. 7. Typical example of the fast convergence of the control parameters (a) η_1 and (b) η_2, as functions of time (length of signal). The first point corresponds to 200 data points in one block. For each next point, the number of data points was increased by 200. The vertical lines show the standard deviations of the inferred values of the control parameters calculated over 1000 runs. The horizontal dashed lines indicate the true values of the parameters. The mixing matrix is defined in Table III. The inferred parameters η_i start from an initial value of $\eta_1=\eta_2=0.2$ and converge quickly to the true values of $\eta_1=0.4$, $\eta_2=0.3$. The coefficients α_i, β_i, γ_i, and d_{ij} are given in Table I. The noise amplitude is $\sqrt{d_1}=\sqrt{d_2}=0.012\,25$.

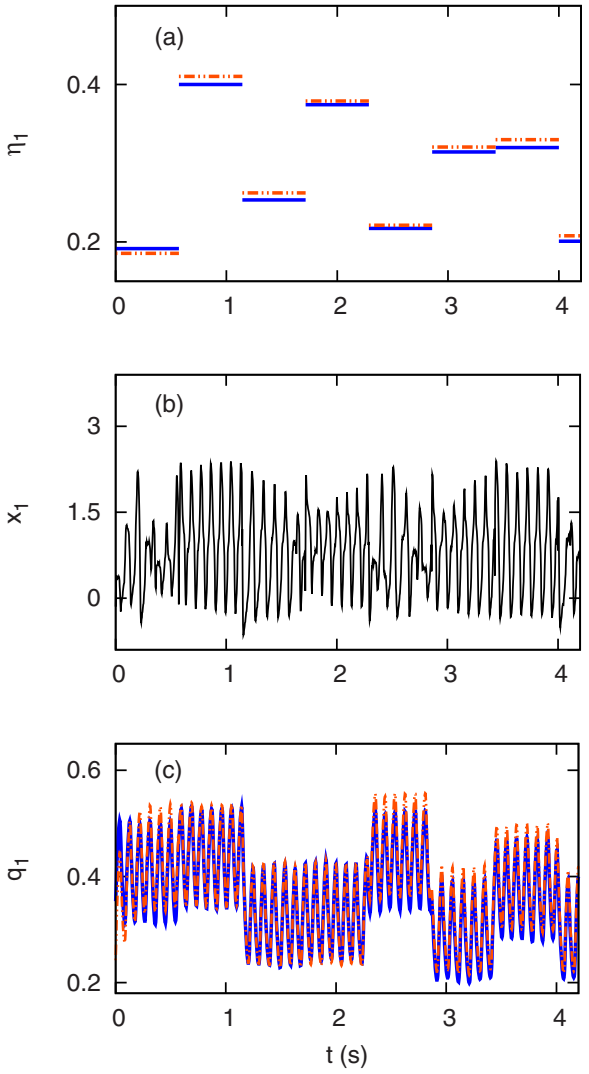

FIG. 8. (Color online) Inference of the parameters of two uncoupled FHN systems mixed by the measurement matrix. It is assumed that η_1 and η_2 change stepwise while all other parameters of the system are fixed and unknown. (a) The inferred values of η_1 (dashed red lines) are compared with their true values (full blue lines). (b) Measured mixed values of the coordinate $x_1(t)$. (c) Inferred values of the coordinate $q_1(t)$ (red dotted line) are compared with its true values (blue solid line). The other parameters are fixed at the values given in Table I. The noise amplitude is $\sqrt{d_1}=\sqrt{d_2}=0.012\,25$.

evident that the time scale for the convergence of η is $\sim$20 ms as compared to the convergence over $\sim$1 s in Fig. 6. It is therefore clear that the computational delay time of $<$500 ms desired for physiological applications can be achieved easily within our Bayesian framework. Next, we consider the efficiency of the method under nonstationary conditions.

IV. NONSTATIONARY DYNAMICS

We consider the situation when all parameters except η_i [Eq. (4)] are fixed at the values given in Table I, but the control parameters η_i are allowed to change, either stepwise or continuously.

A. Stepwise changes of control parameters

1. Unknown parameters

In this section, it is assumed that none of the parameters of the model are known and that they have to be inferred at each step of the measurements. The parameters η_1 and η_2 are allowed to change at random in time in a steplike manner, and remain constant between steps. The time interval between steps is approximately five periods of firing of the action potential and contains one block of data with 20 000 points. Other parameters of the model are fixed at the constant values given in Table I. At each step, we infer all parameters of the model assuming their initial values to be zero and their initial dispersion to be infinity, as already discussed above.

The results of this test are shown in Fig. 8. The inferred values of parameter η_1 are compared with their true values in Fig. 8(a). The time trace of the unknown coordinate $q_1(t)$ is compared with the corresponding reconstructed time trace $\tilde{q}_1(t)$ in Fig. 8(c). The latter time traces were reconstructed as follows. First, the initial coordinates $q_i(t=0)$ and variables

$v_i(t)$ were reconstructed using the inferred measurement matrix $\boldsymbol{X}$ and Eqs. (3) and (10). Second, the variable $\tilde{\mathbf{q}}(t)$ was reconstructed using Eq. (33) of [6],

$$q_i(t=0) = X_{ij}^{-1}\tilde{q}_j(t=0),$$

$$y_i(t) = X_{ij}^{-1}y_j(t),$$

$$\tilde{\mathbf{q}}(t_k) = \gamma h \sum_{r=0}^{k} e^{-\beta(t_k - t_r)}\mathbf{y}(t_r) + e^{-\beta t_k}\mathbf{q}(0) - \frac{h\gamma}{2}[\mathbf{y}(t_k) + e^{-\beta t_k}\mathbf{y}(t_0)]. \quad (17)$$

It can be seen from the figure that the time resolution of the method is of the order of 500 ms even in the case when *none* of the model parameters is known. As mentioned above, however, the time resolution of the method can be improved substantially by considering the other parameter of the model to be known on the time scale of a few seconds (corresponding to their correlation time, see Sec. II) and tracking in time only the time-varying control parameters η_i.

2. Tracking control parameters with known dynamics

We now investigate how fast physiological parameters can be tracked in time. It was shown above (see Sec. III C) that the convergence speed depends on information about the model parameters that is available *a priori*, and that the fastest time resolution can be achieved when all the parameters of the model, except the control parameters η_i, are known. To demonstrate this effect, we now assume that η_1 and η_2 change stepwise at random and remain constant between steps as above, but that all other parameters of the model remain fixed at known values. The time interval between steps is now approximately 0.03 s and contains one block of data with 1000 points. The results of Fig. 9 show that the method can track random, stepwise variations of the control parameters with a time resolution of less than 0.03 s (i.e., smaller by more than two orders of magnitude than in the previous case where all parameters had to be inferred).

B. Continuously varying control parameters with noise

To complete our analysis of the reconstruction of nonstationary dynamics of the physiological model, we now infer smoothly varying parameters η_1 and η_2 with added noise, without knowing any other parameters of the model. The test is performed as follows: (i) all parameters of the model are inferred from the first block (with 30 000 points) of stationary dynamics; (ii) for all other blocks of data, we use acquired information to fix the model parameters constant at the inferred values, and track in time only variations of the control parameters η_i. Each block of data (except the first one) contains 12 000 points and has a time length $t \approx 0.34$ s. The time traces of the unknown variables $q_i(t)$ are reconstructed at every step using Eqs. (17) as explained above. The inferred time evolution of the control parameters η_i is compared with its true variation in Fig. 10. It is evident from the figure that the method allows us to infer the unknown

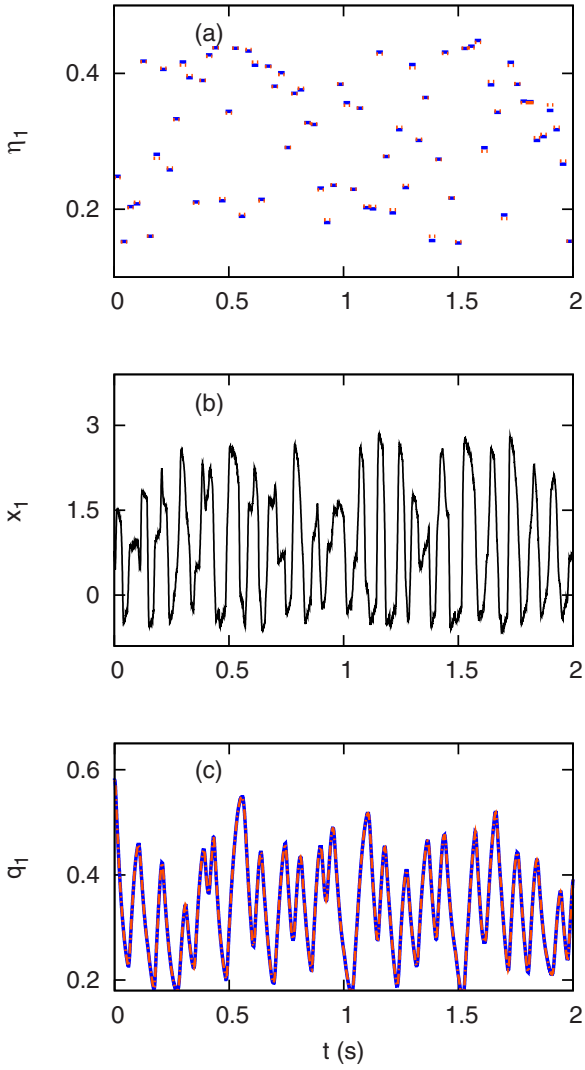

FIG. 9. (Color online) Inference of the model parameters of two uncoupled FHN systems mixed by the measurement matrix. It is assumed that η_1 and η_2 change stepwise while all other parameters of the system are fixed and known. (a) Inferred values η_1 (short elements of red dashed line) are compared with their true values (short elements of full blue line) as a function of time. (b) The time trace of the measured coordinate $x_1(t)$. (c) The time trace of the inferred coordinate $\tilde{q}_1(t)$ (red dotted line) is compared with its true value $q_1(t)$ (blue solid line). The values of the other parameters are fixed, as given in Table I. The noise amplitude is $\sqrt{d_1} = \sqrt{d_2} = 0.012\,25$.

constant parameters of the model, and then also to use this information to track in time the nonstationary control parameters of the system with a time resolution of the order of 0.3 s.

V. CONCLUSION

In summary, we have explored the performance of the Bayesian inferential framework for nonstationary dynamics that we introduced in paper I [6] in relation to physiological applications. We did so by modeling a physiological signal as a set of fast variables y_i, mixed by an unknown measure-

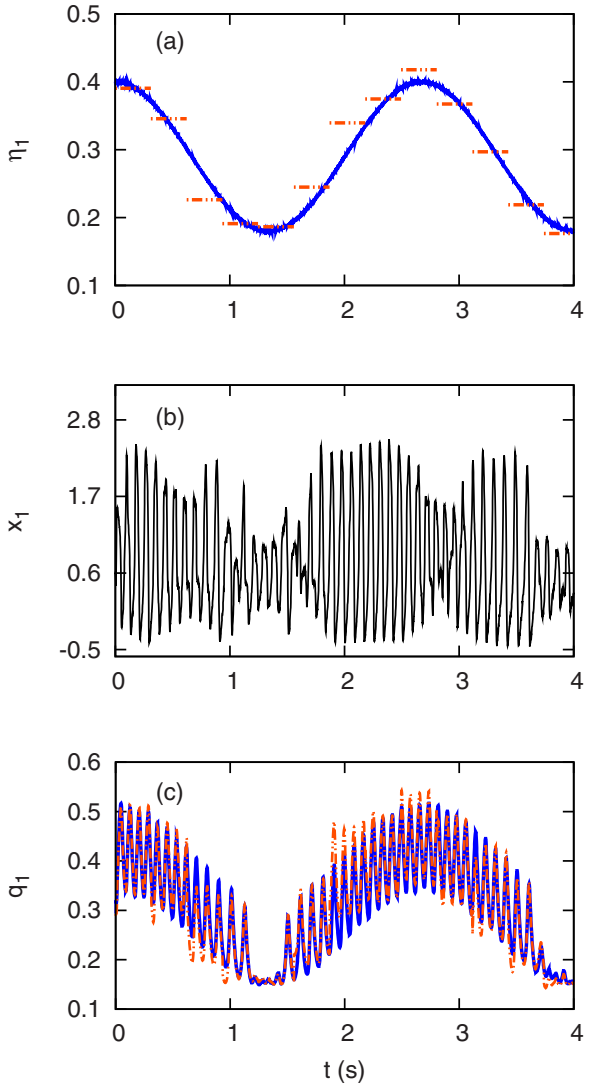

FIG. 10. (Color online) Inference of η_1 and η_2 while smoothly varying in the presence of noise. No prior knowledge of the model parameters is assumed. (a) The inferred values of η_1 (dashed red lines) are compared with their true values (full blue lines). (b) The measured time trace of the mixed coordinate $x_1(t)$. (c) The inferred time trace of the mixed coordinate $\tilde{q}_1(t)$ (dashed red line) is compared with its true value $q_1(t)$ (full blue line). The values of the other parameters are given in Table I. The noise amplitude is $\sqrt{d_1}=\sqrt{d_2}=0.012\,25$.

ment matrix, corresponding to the action potentials of stochastic FHN oscillators. Our goal was to see whether we could track on-line the control parameters η_i of the model, given that these can vary with correlation time $\tau_{\mathrm{cor}} \lesssim 500$ ms. It was assumed that the slow recovery variables of the FHN oscillators were unavailable for measurement and that the correlation time of all other unknown parameters of the model was of the order of 5 s. We have established that the method does indeed facilitate on-line tracking of η_i with a time resolution <0.3 s. This was achieved by embedding the fast on-line tracking of the control parameters within a Bayesian learning framework for the more slowly varying parameters of the system with a time resolution <1 s.

We showed that the time resolution of the method is determined by the eigenvalues of the matrix $\hat{\boldsymbol{\Xi}}^{-1}=\hat{\mathbf{D}}\otimes\hat{\boldsymbol{\Phi}}_k^{-1}$, and therefore depends essentially on the choice and scale of the base functions. Note that, while the eigenvalues of $\hat{\mathbf{D}}$ are intrinsic to the system, the choice and scale of the base functions can be controlled by the researcher. Specifically, we demonstrated that by accumulating *a priori* information about slowly varying model parameters, one can enhance the time resolution of the control parameters by an order of magnitude.

Several limitations of the method should be borne in mind in adapting it to any particular application. As we have already mentioned, fast online applications require that measurement noise be small. In addition, it was assumed that the equations for the hidden variables are linear and deterministic. The latter limitations can be removed, at least partially, by writing the equation for the hidden variables in the more general form $\dot{q}=f(q)+g(y)$, where the homogeneous equation $\dot{q}=f(q)$ is integrable and the nonlinear function of the measurable variable $g(y)$ is arbitrary. One can then proceed in exactly the same way as described in the present paper. Furthermore, the method can be extended to encompass the case of an integrable stochastic differential equation for the hidden variables. To do so, a stochastic integral must be added to the right-hand sides of the equations of reduced dynamics. Finally, the method can be applied to the case in which the dynamics of the system jumps at random between different states, as, for example, in gating dynamics. Note, however, that if the different states are characterized by different dynamical models, then the solution of the inference problem can be obtained more generally within the framework of a hybrid probabilistic approach, as will be described in more detail elsewhere. We note that the method is also useful when the low-dimensional dynamics is only a rough approximation to the actual multidimensional complex dynamics of the system. The latter situation is often the case in physiological and aerospace applications [21,22].

We conclude, therefore (see also [6]), that the results obtained are of broad interdisciplinary interest. They were recently shown to be particularly useful in medical applications [20] and for the development of prognostics and diagnostics techniques in aerospace applications [21,22]. The method can readily be extended to encompass systems with multiplicative and colored noise, and efforts toward these ends are already in progress.

ACKNOWLEDGMENTS

We are grateful to the Engineering and Physical Sciences Research Council (UK) and NASA for financial support, and to A. Stefanovska for valuable discussions.

[1] R. Mukkamala and R. J. Cohen, Am. J. Physiol. Heart Circ. Physiol. **281**, H2714 (2001).
[2] S. Lu and K. H. Chon, IEEE Trans. Signal Process. **51**, 3020 (2003).
[3] A. B. Schwartz, X. T. Cui, D. J. Weber, and D. W. Moran, Neuron **52**, 205 (2006).
[4] F. Lotte *et al.*, J. Neural Eng. **4**, R1 (2007).
[5] S. Eyal and S. Akselrod, Methods Inf. Med. **39**, 118 (2000).
[6] D. G. Luchinsky, V. N. Smelyanskiy, A. Duggento, and P. V. E. McClintock, preceding paper, Phys. Rev. E **77**, 061105(2008).
[7] R. FitzHugh, Biophys. J. **1**, 445 (1961).
[8] J. Nagumo, S. Animoto, and S. Yoshizawa, Proc. IRE **50**, 2061 (1962).
[9] A. T. Winfree, *The Geometry of Biological Time* (Springer-Verlag, New York, 1980).
[10] J. Keener and J. Sneyd, *Mathematical Physiology* (Springer-Verlag, New York, 1998).
[11] E. N. Best, Biophys. J. **27**, 87 (1979).
[12] J. Rogers and A. McCulloch, IEEE Trans. Biomed. Eng. **41**, 743 (1994).
[13] R. R. Aliev and A. V. Panfilov, J. Theor. Biol. **81**, 33 (1996).
[14] P. Chen, SIAM J. Math. Anal. **23**, 81 (1992).
[15] O. Berenfeld and S. Abboud, Med. Eng. Phys. **18**, 615 (1996).
[16] D. Bullock, P. Cisek, and S. Grossberg, Cereb. Cortex **8**, 48 (1998).
[17] S. Rajasekar and M. Lakshmanan, J. Theor. Biol. **166**, 275 (1994).
[18] R. Mannella, Int. J. Mod. Phys. C **13**, 1177 (2002).
[19] D. M. Bates and D. G. Watts, *Nonlinear Regression and Its Applications* (Wiley, New York, 1988).
[20] D. G. Luchinsky, M. M. Millonas, V. N. Smelyanskiy, A. Pershakova, A. Stefanovska, and P. V. E. Mcclintock Phys. Rev. E **72**, 021905 (2005).
[21] V. V. Osipov, D. G. Luchinsky, V. N. Smelyanskiy, and D. A. Timucin, *Proceedings of the AIAA/ASME/SAE/ASEE Joint Propulsion Conference and Exhibit, AIAA Conference Proceedings* (AIAA, Cincinnati, OH, 2007), AIAA 2007-5823.
[22] D. G. Luchinsky, V. N. Smelyanskiy, V. V. Osipov, D. A. Timucin, and S.-H Lee, *Proceedings of the AIAA Infotech@Aerospace 2007 Conference and Exhibit, AIAA Conference Proceedings* (AIAA, Robnert Park, CA, 2007), AIAA 2007-2829.